

# F-wave versus P-wave Superconductivity in Organic Conductors

R. W. Cherng<sup>†</sup> and C. A. R. Sá de Melo

*School of Physics, Georgia Institute of Technology, Atlanta Georgia 30332*

(Dated: October 31, 2018)

Current experimental results suggest that some organic quasi-one-dimensional superconductors exhibit triplet pairing symmetry. Thus, we discuss several potential triplet order parameters for the superconducting state of these systems within the functional integral formulation. We compare weak spin-orbit coupling  $f_{xyz}$ ,  $p_x$ ,  $p_y$  and  $p_z$  symmetries via several thermodynamic quantities. For each symmetry, we analyse the temperature dependences of the order parameter, condensation energy, specific heat, and superfluid density tensor.

PACS numbers: 74.70.Kn

Recent NMR experiments in the organic conductor (Bechgaard salt)  $(\text{TMTSF})_2\text{PF}_6$ <sup>1,2</sup> in combination with earlier upper critical field ( $H_{c2}$ ) measurements<sup>3</sup> indicate that this system may be an unconventional triplet superconductor at low temperature ( $T$ ). Lee *et. al.*<sup>1,2</sup> observed that there is **no**  $^{77}\text{Se}$  Knight shift for fields  $\mathbf{H} \parallel \mathbf{b}'$  ( $P \approx 6$  kbar) and  $\mathbf{H} \parallel \mathbf{a}$  ( $P \approx 7$  kbar). This indicates that the spin susceptibilities in the superconducting state are  $\chi_a \approx \chi_N$ , and  $\chi_{b'} \approx \chi_N$ , where  $\chi_N$  is the normal state susceptibility. Their measurements suggest that the  $\mathbf{d}$ -vector order parameter for triplet superconductivity is pointing along the  $\mathbf{c}^*$  axis. Unfortunately, the spin susceptibility in the superconducting state for fields along the  $\mathbf{c}^*$  axis could not be measured because the upper critical field ( $H_{c2}^*$ ) was exceeded before a signal could be detected. Since the low  $T$  dependence of  $\chi_{c^*}(T)$  is not accessible experimentally, it may not be possible to use this technique to decipher the node structure of the triplet order parameter. The symmetry of the order parameter in the sister compound  $(\text{TMTSF})_2\text{ClO}_4$  was preliminarily explored in the thermal conductivity experiments of Belin and Behnia<sup>4</sup> (BB). They indicated that their data was inconsistent with the existence of gap nodes at the Fermi surface as suggested by Takigawa *et. al.*<sup>5</sup>. These results combined with upper critical field measurements<sup>6,7</sup> seem to suggest a fully gapped triplet state in  $(\text{TMTSF})_2\text{ClO}_4$ . However, detailed  $^{77}\text{Se}$  NMR experiments seem to be lacking for  $(\text{TMTSF})_2\text{ClO}_4$ . These experiments were inspired by early suggestions of triplet superconductivity in the Bechgaard salts<sup>8,9,10,11</sup>, but following these new experimental developments theoretical efforts intensified<sup>12,13,14,15,16</sup>. Lebed, Machida, and Ozaki (LMO)<sup>12</sup> proposed a “p-wave” triplet order parameter for  $(\text{TMTSF})_2\text{PF}_6$ , where the  $\mathbf{d}$ -vector had a strong component along the  $\mathbf{a}$  direction, thus producing a strongly anisotropic spin susceptibility with  $\chi_a \ll \chi_N$  and  $\chi_{b'} \approx \chi_N$ . A fully gapped singlet “d-wave” order parameter for  $(\text{TMTSF})_2\text{ClO}_4$  was proposed by Shimahara<sup>13</sup>, while gapless triplet “f-wave” superconductivity for  $(\text{TMTSF})_2\text{PF}_6$  was proposed by Kuroki, Arita, and Aoki (KAA)<sup>14</sup>. Duncan, Vaccarella and Sá de Melo (DVS)<sup>15,16</sup> performed a detailed group theoretical analysis and suggested that a weak spin-orbit fully gapped triplet “ $p_x$ -wave” order parameter, where  $\chi_a \approx \chi_N$  and

$\chi_{b'} \approx \chi_N$ <sup>17,18</sup>, would be a good candidate for superconductivity in Bechgaard salts.

In this paper, we consider only triplet states corresponding to weak spin-orbit coupling, since in  $(\text{TMTSF})_2\text{X}$  the heaviest element is  $^{77}\text{Se}$ . Within the orthorhombic ( $D_{2h}$ ) group, this limits the number of possibilities for the order parameter<sup>15,16</sup> to four symmetries,  $p_x$ ,  $p_y$ ,  $p_z$ ,  $f_{xyz}$ . For each one of these symmetries, we calculate the temperature dependences of the order parameter, condensation energy, entropy, specific heat, and superfluid density tensor.

We study single band quasi-one-dimensional systems in an orthorhombic lattice with dispersion relation

$$\epsilon_{\mathbf{k}} = -|t_x| \cos(k_x a_x) - |t_y| \cos(k_y a_y) - |t_z| \cos(k_z a_z),$$

where  $|t_x| \gg |t_y| \gg |t_z|$ . Furthermore,  $a_x$ ,  $a_y$  and  $a_z$  in our notation correspond to the unit cell lengths along the crystallographic directions  $\mathbf{a}$ ,  $\mathbf{b}'$ , and  $\mathbf{c}^*$  respectively. We work with the Hamiltonian  $H = H_{kin} + H_{int}$ , where the kinetic energy part is  $H_{kin} = \sum_{\mathbf{k}, \alpha} \xi_{\mathbf{k}} \psi_{\mathbf{k}, \alpha}^\dagger \psi_{\mathbf{k}, \alpha}$ , with  $\xi_{\mathbf{k}} = \epsilon_{\mathbf{k}} - \mu$  and the interaction part is

$$H_{int} = \frac{1}{2} \sum_{\mathbf{k}, \mathbf{k}', \mathbf{q}} \sum_{\alpha \beta \gamma \delta} V_{\alpha \beta \gamma \delta}(\mathbf{k}, \mathbf{k}') b_{\alpha \beta}^\dagger(\mathbf{k}, \mathbf{q}) b_{\gamma \delta}(\mathbf{k}', \mathbf{q}) \quad (1)$$

with  $b_{\alpha \beta}^\dagger(\mathbf{k}, \mathbf{q}) = \psi_{-\mathbf{k}+\mathbf{q}/2, \alpha}^\dagger \psi_{\mathbf{k}+\mathbf{q}/2, \beta}^\dagger$ , where  $\alpha$ ,  $\beta$ ,  $\gamma$  and  $\delta$  are spin indices and  $\mathbf{k}$ ,  $\mathbf{k}'$  and  $\mathbf{q}$  represent linear momenta. We use units where  $\hbar = k_B = 1$ .

In the case of weak spin-orbit coupling and triplet pairing, the model interaction tensor can be chosen to be

$$V_{\alpha \beta \gamma \delta}(\mathbf{k}, \mathbf{k}') = V_\Gamma h_\Gamma(\mathbf{k}, \mathbf{k}') \phi_\Gamma(\mathbf{k}) \phi_\Gamma^*(\mathbf{k}') \Gamma_{\alpha \beta \gamma \delta}, \quad (2)$$

where  $\Gamma_{\alpha \beta \gamma \delta} = \mathbf{v}_{\alpha \beta} \cdot \mathbf{v}_{\gamma \delta}^\dagger / 2$  with  $\mathbf{v}_{\alpha \beta} = (i\sigma\sigma_y)_{\alpha \beta}$ .  $V_\Gamma$  is a prefactor with dimensions of energy which characterizes a given symmetry. Furthermore, the term  $h_\Gamma(\mathbf{k}, \mathbf{k}') \phi_\Gamma(\mathbf{k}) \phi_\Gamma^*(\mathbf{k}')$  contains the momentum and symmetry dependence of the interaction of the irreducible representation  $\Gamma$  with basis function  $\phi_\Gamma(\mathbf{k})$  and  $\phi_\Gamma^*(\mathbf{k}')$  representative of the orthorhombic group ( $D_{2h}$ ).

We use the functional integration method to write down the partition function  $Z = \int \mathcal{D}[\psi^\dagger, \psi] \exp[S]$  where

$S = \int d\tau \left[ \sum_{\mathbf{k}, \alpha} \psi_{\mathbf{k}, \alpha}^\dagger(\tau) (-\partial_\tau) \psi_{\mathbf{k}, \alpha}(\tau) - H(\psi^\dagger, \psi) \right]$ . We treat  $H_{int}$  in the zero center of mass momentum ( $\mathbf{q} = \mathbf{0}$ ) pairing approximation. Furthermore, since we are mostly interested in symmetry aspects we take  $h_\Gamma(\mathbf{k}, \mathbf{k}') = 1$ . We introduce the Gaussian integral  $I_G = \int d[\mathcal{D}_i^\dagger, \mathcal{D}_i] \exp[-Q_G]$ , where  $Q_G = \int d\tau \sum_{\mathbf{k}, \mathbf{k}'} \mathcal{D}_i^\dagger(\mathbf{k}, \tau) \mathcal{D}_i(\mathbf{k}', \tau) / V_\Gamma$ . The shift transformation  $\mathcal{D}_i^\dagger(\mathbf{k}, \tau) \rightarrow \mathcal{D}_i^\dagger(\mathbf{k}, \tau) + V_\Gamma v_{\alpha\beta, i} \phi_\Gamma(\mathbf{k}) \psi_{-\mathbf{k}, \alpha}^\dagger \psi_{\mathbf{k}, \beta}^\dagger$  eliminates  $H_{int}$  and integration over the fermionic degrees of freedom results in the effective action

$$S_{\text{eff}} = -Q_G - Tr \ln [\mathbf{M}/2], \quad (3)$$

where  $\mathbf{M}$  is a  $2 \times 2$  block diagonal matrix of the form

$$\begin{pmatrix} [\partial_\tau + \xi_{\mathbf{k}}] \delta_{\alpha\beta} & \sum_{\mathbf{k}'} \mathcal{D}_i(\mathbf{k}', \tau) v_{\beta\alpha, i} \phi_\Gamma(\mathbf{k}) \\ \sum_{\mathbf{k}'} \mathcal{D}_i^\dagger(\mathbf{k}', \tau) v_{\alpha\beta, i} \phi_\Gamma^*(\mathbf{k}) & [-\partial_\tau - \xi_{\mathbf{k}}] \delta_{\alpha\beta} \end{pmatrix}.$$

Thus,  $Z = \int d[\mathcal{D}_i^\dagger, \mathcal{D}_i] \exp[S_{\text{eff}}]$ . At the saddle point approximation  $\mathcal{D}_i(\mathbf{k}, \tau)$  is taken to be  $\tau$  independent, and  $\sum_{\mathbf{k}'} \mathcal{D}_i(\mathbf{k}') \equiv \hat{\eta}_i \Delta_\Gamma$ . The order parameter equation is obtained from the stationary condition  $\delta S_{\text{eff}}^{(0)} / \delta \mathcal{D}_i^\dagger = 0$  leading to

$$1 = - \sum_{\mathbf{k}} V_\Gamma |\phi_\Gamma(\mathbf{k})|^2 \tanh(E_{\mathbf{k}}/2T) / 2E_{\mathbf{k}}, \quad (4)$$

where  $E_{\mathbf{k}} = \sqrt{\xi_{\mathbf{k}}^2 + |\Delta_\Gamma|^2 |\phi_\Gamma(\mathbf{k})|^2}$ . The number equation is obtained from  $N = -\partial \Omega_0 / \partial \mu$ , where  $\Omega_0 = -T S_{\text{eff}}^{(0)}$  is the saddle point thermodynamic potential, and results in

$$N = \sum_{\mathbf{k}} n_{\mathbf{k}}, \quad (5)$$

where  $n_{\mathbf{k}} = [1 - \xi_{\mathbf{k}} \tanh(E_{\mathbf{k}}/2T) / E_{\mathbf{k}}]$  is the momentum distribution. These two equations must be solved self-consistently, and quite generally they are correct even in the strong coupling (or low density) regime provided that  $T \ll T_c$ . Corrections to  $\Omega$  and  $N$  can be obtained by considering Gaussian fluctuations. Writing  $\mathcal{D}_i(\mathbf{k}, \tau) = \mathcal{D}_i(\mathbf{k}) + \delta \mathcal{D}_i(\mathbf{k}, \tau)$  and expanding  $Tr \ln [\mathbf{M}]$  to quadratic order in  $\delta \mathcal{D}_i(\mathbf{k}, \tau)$  results in the effective action  $S_{\text{eff}} = S_{\text{eff}}^{(0)} - Tr [\mathbf{M}^{-1} \mathbf{U}]^2 / 2$ , where  $\mathbf{U}$  is a  $2 \times 2$  block matrix that contains only off-diagonal elements, with  $U_{12} = \sum_{\mathbf{k}'} \delta \mathcal{D}_i(\mathbf{k}', \tau) v_{\beta\alpha, i} \phi_\Gamma(\mathbf{k})$  and  $U_{21} = U_{12}^\dagger$ . These corrections are important for small carrier density (or  $T_c \sim E_F$ ), however, in the BCS limit of high carrier density (or  $T_c \ll E_F$ ), discussed here, these corrections are negligible for  $N$ , but are important for  $\Omega$  only when  $T \ll T_c$ . For Bechgaard salts,  $T_c \approx 1.5$  K and  $E_F \approx 3,071$  K (with respect to the bottom of the band). The vector  $\mathcal{D}_i$  is related to the standard  $\mathbf{d}$ -vector via the relation  $d_i(\mathbf{k}) = \sum_{\mathbf{k}'} \mathcal{D}_i(\mathbf{k}') \phi_\Gamma(\mathbf{k})$ . In the  $D_{2h}$  point group all representations are one dimensional and non-degenerate<sup>15,16</sup>, which means that the  $\mathbf{d}$ -vector in momentum space for unitary triplet states in the weak spin-orbit coupling limit is characterized by one

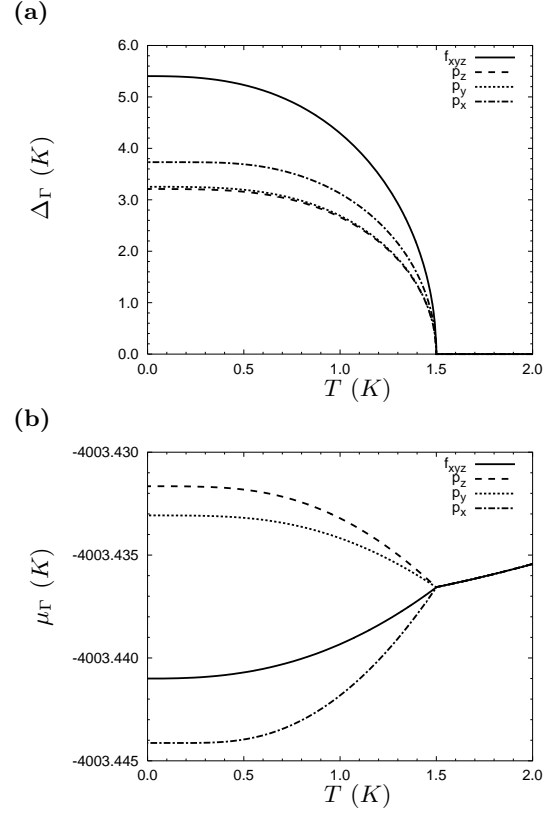


FIG. 1: Temperature dependence for (a)  $\Delta_\Gamma$  and (b)  $\mu_\Gamma$  in thermal units (K). Notice that  $\mu_\Gamma$  is nearly  $T$  independent.

of the four states: (1)  ${}^3A_{1u}(a)$ , with  $\mathbf{d}(\mathbf{k}) = \hat{\eta} \Delta_{f_{xyz}} XYZ$  (“ $f_{xyz}$ ” state); (2)  ${}^3B_{1u}(a)$ , with  $\mathbf{d}(\mathbf{k}) = \hat{\eta} \Delta_{p_z} Z$  (“ $p_z$ ” state); (3)  ${}^3B_{2u}(a)$ , with  $\mathbf{d}(\mathbf{k}) = \hat{\eta} \Delta_{p_y} Y$  (“ $p_y$ ” state); (4)  ${}^3B_{3u}(a)$ , with  $\mathbf{d}(\mathbf{k}) = \hat{\eta} \Delta_{p_x} X$  (“ $p_x$ ” state). Since, the Fermi surface touches the Brillouin zone boundaries the functions  $X$ ,  $Y$ , and  $Z$  need to be periodic and can be chosen to be  $X = \sin(k_x a_x)$ ,  $Y = \sin(k_y a_y)$ , and  $Z = \sin(k_z a_z)$ . The unit vector  $\hat{\eta}$  defines the direction of  $\mathbf{d}(\mathbf{k})$ . The  $T$  dependence of  $\Delta_\Gamma$  and  $\mu_\Gamma$  for  $f_{xyz}$ ,  $p_x$ ,  $p_y$  and  $p_z$  symmetries are shown in Fig. 1. The parameters used are  $|t_x| = 5800$  K,  $|t_y| = 1226$  K and  $|t_z| = 48$  K, and  $N/N_{max} = 1/4$  (quarter-filling). The minimum value of the dispersion  $\epsilon(\mathbf{k})$  is  $\epsilon_{min} = -7,074$  K, while the maximum is  $\epsilon_{max} = +7,074$  K. In order to make direct comparison between different symmetries we choose  $T_c = 1.5$  K for all symmetries. This requirement forces the interaction strength prefactors to be  $V_{f_{xyz}} \approx -12,577$  K;  $V_{p_z} \approx -2,910$  K;  $V_{p_y} \approx -3,025$  K;  $V_{p_x} \approx -3,208$  K. Notice in Fig. 1a that  $\Delta_{f_{xyz}} > \Delta_{p_x} > \Delta_{p_y} > \Delta_{p_z}$  for all  $T < T_c$ , and that  $\mu_\Gamma$  is largely independent of  $T$ , however, the condition  $\mu_{p_z} > \mu_{p_y} > \mu_{f_{xyz}} > \mu_{p_x}$  applies for all  $T < T_c$ . The relative stability of these phases can be studied via the condensation energy  $\Delta \mathcal{F}_\Gamma = \mathcal{F}_\Gamma(T) - \mathcal{F}_N(T)$ , where  $\mathcal{F}_\Gamma(T)$  and  $\mathcal{F}_N(T)$  are the Helmholtz free energies of the superconducting state with symmetry  $\Gamma$  and of the normal state, respectively.  $\Delta \mathcal{F}_\Gamma$  is calculated us-

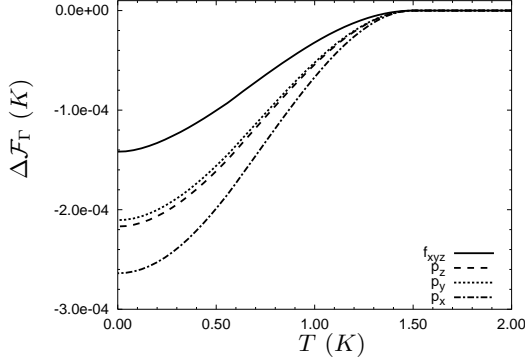


FIG. 2: Temperature dependence of the condensation energy  $\Delta\mathcal{F}_\Gamma$  in thermal units (K).

ing  $\mathcal{F} = \Omega + \mu N$ . Fig. 2 shows  $\Delta\mathcal{F}_\Gamma$  for the  $f_{xyz}$ ,  $p_x$ ,  $p_y$  and  $p_z$  symmetries. Notice that  $\Delta\mathcal{F}_\Gamma$  are very small, are expressed in thermal units, and obey the relations  $|\Delta\mathcal{F}_{p_x}| > |\Delta\mathcal{F}_{p_z}| > |\Delta\mathcal{F}_{p_y}| > |\Delta\mathcal{F}_{f_{xyz}}|$  for  $T < T_c$ . The  $p_x$  symmetry which has a full gap, has also the largest (negative)  $\Delta\mathcal{F}_\Gamma$ . The values of  $\Delta\mathcal{F}_{p_z}$  and  $\Delta\mathcal{F}_{p_y}$  are very close reflecting that the  $p_z$  and  $p_y$  symmetries have lines of nodes at  $Z = 0$  and  $Y = 0$ , respectively. Lastly, the  $f_{xyz}$  symmetry has double zeros at  $Z = 0$  **and**  $Y = 0$  and has line nodes at  $Z = 0$  **or**  $Y = 0$ , which are costly in condensation energy. This confirms the general expectation that a fully gapped (nodeless) superconducting phase ( $p_x$ ) is more likely to win over competing phases which have nodes ( $p_y$ ,  $p_z$  and  $f_{xyz}$ ).

Since  $\Omega_0$  is only a function of  $|\mathbf{d}(\mathbf{k})|^2$  (recall that  $|\mathbf{d}(\mathbf{k})|^2 = |\Delta_\Gamma|^2 |\phi_\Gamma(\mathbf{k})|^2$ ) the vector nature of  $\mathbf{d}(\mathbf{k})$  does not appear explicitly in thermodynamic properties. However, the node structure of triplet order parameters can be probed by a specific heat measurement. The specific heat  $C_\Gamma = -T\partial^2\mathcal{F}_\Gamma/\partial T^2$  is

$$C_\Gamma = \frac{2}{T^2} \sum_{\mathbf{k}} P(E_{\mathbf{k}}) \left[ E_{\mathbf{k}}^2 + T\xi_{\mathbf{k}} \frac{\partial \mu}{\partial T} - \frac{T}{2} \frac{\partial |\mathbf{d}(\mathbf{k})|^2}{\partial T} \right],$$

where  $P(E_{\mathbf{k}}) = f(E_{\mathbf{k}})[1 - f(E_{\mathbf{k}})]$ . The results for  $C_\Gamma$  can be seen in Fig. 3, and analysed as follows. The specific heat jump at  $T_c = 1.5$  K is characterized by the parameter  $\theta_\Gamma = C_{S,\Gamma}(T_c)/C_N(T_c) - 1$ , which takes values  $\theta_{f_{xyz}} = 0.5596$ ,  $\theta_{p_z} = 0.9733$ ,  $\theta_{p_y} = 0.9358$ , and  $\theta_{p_x} = 1.2001$ . The corresponding singlet s-wave value is  $\theta_s = 1.4604$ . An analysis of  $C_\Gamma$  at low  $T$  is also important in distinguishing possible weak spin-orbit triplet phases. Using the fact that  $\partial\mu/\partial T \approx 0$ ,  $\partial|\mathbf{d}(\mathbf{k})|^2/\partial T \approx 0$  at low  $T$ , then  $C_\Gamma \approx 2T \int_0^\infty dw w^2 \text{sech}^2(w) N(2Tw)$ , where  $w \equiv \omega/2T$  and  $N(\omega) = 2 \sum_{\mathbf{k}} \delta(\omega - E_{\mathbf{k}})$  is the auxiliary density of states. This leads to  $C_{f_{xyz}} = (T/T_{f_{xyz}})^2 \log(K_3 \Delta_{f_{xyz}}/T)$ , where the temperature scale  $T_{f_{xyz}}^{-2} = [2(\Delta_{f_{xyz}} t_x)^{-1} D/\pi\kappa] \gamma(3)$ , with  $D = 16/[\pi|\sin(x)|]$ ,  $\gamma(m) = \int_0^\infty dw w^m \text{sech}^2(w)$ ,  $\kappa = \sqrt{1 - (\mu/t_x)^2}$  and  $K_m = \exp[\int_0^\infty dw w^m \text{sech}^2(w) \log[4w^{-1}\kappa]/\gamma(m)]$ .

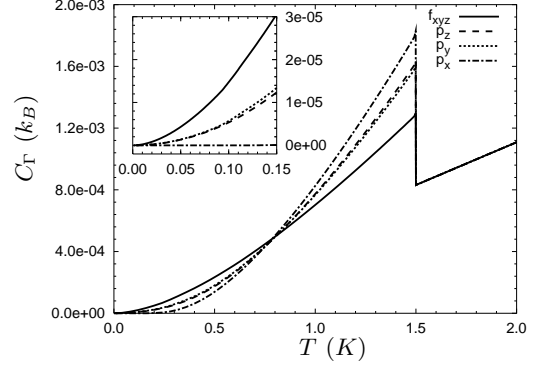


FIG. 3: Temperature dependence of specific heat  $C_\Gamma$  in units of  $k_B$ . Inset shows low  $T$  behavior.

This  $T$  dependence of  $C_{f_{xyz}}$  is a reflexion of the the behavior of  $N(\omega) = \alpha(\omega/\Delta_0) \log(\beta\Delta_0/\omega)$  at small  $\omega$ , where  $\alpha$  and  $\beta$  are constants. The presence of the logarithmic term results from the large number of low-energy states surrounding the double zeros of the order parameter at the relatively flat Fermi surface. The  $p_z$  and  $p_y$  symmetries, however, have very different behaviors at low  $T$ , given that both order parameters have lines of nodes at the Fermi surface, but no double zeros. In this case, the specific heats behave as  $C_{p_z} = (T/T_{p_z})^2$ , and  $C_{p_y} = (T/T_{p_y})^2$ , where  $T_{p_j}^{-2} = [\Delta_{p_j}|t_x|]^{-1} D\gamma(3)$ , for  $(p_j = p_z \text{ or } p_y)$ . Lastly,  $C_{p_x} = (T_{p_x}/T)^{1/2} \exp(-\omega_0/T)$ , where  $\omega_0 = \Delta_{p_x} \sqrt{1 - [(|t_y| + |t_z| - \mu)/|t_x|]^2}$  and  $T_{p_x}^{1/2} = AB\gamma(1/2)$ , with  $A = 2(\omega_0)^{7/2}/[\pi^2|\sin(x)|\Delta_{p_x}^2(|t_y| + |t_z| - \mu)]$ ,  $B = [(t_x^2 - \Delta_{p_x}^2)/(t_y t_z)]^{1/2}$ . Notice that  $C_{p_x}$  is exponentially suppressed at low  $T$  due to the presence of a full gap in the excitation spectrum, however the exponential prefactor behaves as  $T^{-1/2}$ , which differs from the  $T^{-3/2}$  behavior of the prefactor in the singlet s-wave case. This difference arises because  $N(\omega)$  in the  $p_x$  case has a square root dependence in the vicinity of the gap edge,  $N_{p_x} \sim \sqrt{\omega - \omega_{0,p_x}}$ , while in the s-wave case  $N(\omega)$  has a square root singularity near the gap edge  $N_s \sim 1/\sqrt{\omega - \omega_{0,s}}$ . The Gaussian correction  $\Omega_G$  to  $\Omega_0$  leads to collective modes at low  $T$  with anisotropic dispersions  $\omega = c_\Gamma(\theta, \phi)|\mathbf{q}|$  for all symmetries. These modes give a symmetry independent  $T^2$  contribution to  $C_\Gamma$ , but the prefactor is symmetry dependent. This collective mode contribution is characteristic of neutral superfluids. However, in real charged superconductors that may become plasmonized, and thus gapped. The temperature dependence of the superfluid density tensor  $\rho_{ij}(T)$  can also be used to distinguish different weak spin-orbit triplet phases. This tensor is directly associated with phase twists of the  $U(1)$  phase of the  $\mathbf{d}$ -vector. Take  $\mathbf{d}(\mathbf{k}) \rightarrow \mathbf{d}(\mathbf{k}) \exp[i\phi(\mathbf{k})]$  and expand  $S_{\text{eff}}$  in powers of  $\phi(\mathbf{k})$  about the saddle point with  $\phi(\mathbf{k}) = 0$ . The resulting action  $\Delta S = S_{\text{eff}}(\phi) - S_{\text{eff}}(\phi = 0)$  is  $\Delta S =$

$-V/2 \sum \phi(\mathbf{k})\phi(-\mathbf{k})k_i k_j \rho_{ij}$ , with

$$\rho_{ij}(T) = \frac{1}{V} \sum_{\mathbf{k}} [n_{\mathbf{k}} \partial_i \partial_j \xi_{\mathbf{k}} - Y_{\mathbf{k}} \partial_i \xi_{\mathbf{k}} \partial_j \xi_{\mathbf{k}}], \quad (6)$$

where  $n_{\mathbf{k}}$  is the momentum distribution, and  $Y_{\mathbf{k}} = (2T)^{-1} \text{sech}^2(E_{\mathbf{k}}/2T)$  is the Yoshida distribution. In Fig. 4 we show the  $T$  dependence of  $\rho_{ij}$ . In the case of the  $D_{2h}$  group only diagonal components  $\rho_{ii}$  exist, but they are highly anisotropic due to the quasi-one-dimensionality of  $\xi_{\mathbf{k}}$ . The low  $T$  behavior of  $\Delta\rho_{ii} \equiv [\rho_{ii}(T)/\rho_{ii}(0) - 1]$  is shown in the inset of Fig. 4. At low  $T$ , the main contributions to  $\Delta\rho_{ii}$  come from the term containing  $Y_{\mathbf{k}}$ . For the  $p_x$  symmetry,  $\Delta\rho_{xx} = -(T/T_{p_x}^x)^{1/2} \exp(-\omega_0/T)$ ,  $\Delta\rho_{yy} = -(T/T_{p_x}^y)^{3/2} \exp(-\omega_0/T)$ ,  $\Delta\rho_{zz} = -(T/T_{p_x}^z)^{3/2} \exp(-\omega_0/T)$ , where  $T_{p_x}^i$  are characteristic temperatures. Notice the exponential behavior due to presence of a full gap. Furthermore, notice that the  $T$  dependence of the prefactor of  $\Delta\rho_{xx}$  is different from  $\Delta\rho_{yy}$  and  $\Delta\rho_{zz}$  due to the highly anisotropic Fermi surface of these systems, i.e., the velocity  $v_x = \partial_x \xi_{\mathbf{k}}$  does not vanish anywhere at the Fermi surface. For the  $p_y$  symmetry,  $\Delta\rho_{xx} = -T/T_{p_y}^x$ ,  $\Delta\rho_{yy} = -(T/T_{p_y}^y)^3$ , and  $\Delta\rho_{zz} = -T/T_{p_y}^z$ . Notice the  $T^3$  power law for  $\Delta\rho_{yy}$ , which results from the simultaneous contribu-

tion from the lines of nodes of  $\mathbf{d}_{p_y}$  and the zeros of  $v_y = \partial_y \xi_{\mathbf{k}}$ . Similar behavior is found also for the  $p_z$  symmetry,  $\Delta\rho_{xx} = -(T/T_{p_z}^x)$ ,  $\Delta\rho_{yy} = -(T/T_{p_z}^y)$ , and  $\Delta\rho_{zz} = -(T/T_{p_z}^z)^3$ . In the  $p_z$  case, however, the  $T^3$  dependence appears in  $\Delta\rho_{zz}$ . Finally for the  $f_{xyz}$  symmetry,  $\Delta\rho_{xx} = -(T/T_{f_{xyz}}^x) \log(K_1 \Delta_{f_{xyz}}/T)$ ,  $\Delta\rho_{yy} = -T/T_{f_{xyz}}^y$ , and  $\Delta\rho_{zz} = -T/T_{f_{xyz}}^z$ . The logarithmic dependence on  $\Delta\rho_{xx}$  originates from the node structure of  $\mathbf{d}_{f_{xyz}}$  and from a non-vanishing  $v_x$  at the Fermi surface. Notice that the logarithmic dependence is absent on  $\Delta\rho_{yy}$  and  $\Delta\rho_{zz}$ , because the zeros of  $v_y$  and  $v_z$  cancel it out. The  $T$  dependence of  $\rho_{ii}(T)$  can be measured via penetration depth experiments.

In summary, we studied several properties of organic quasi-one-dimensional conductors (Bechgaard salts) which are strong candidates for triplet superconductivity. We compared weak spin-orbit coupling symmetries  $f_{xyz}$ ,  $p_x$ ,  $p_y$  and  $p_z$  via several thermodynamic quantities. For each symmetry, we analysed the temperature dependences of the order parameter, condensation energy, specific heat, and superfluid density tensor. We would like to thank NSF (Grant No. DMR-9803111) for support. <sup>†</sup>Present address: Department of Physics, Massachusetts Institute of Technology, Cambridge, MA 02139-4307.

<sup>1</sup> I. J. Lee, D. S. Chow, W. G. Clark, M. J. Strouse, M. J. Naughton, P. M. Chaikin, and S. E. Brown (2000), cond-mat/0001332.

<sup>2</sup> I. J. Lee, S. E. Brown, W. G. Clark, M. J. Strouse, M. J. Naughton, W. Kang, and P. M. Chaikin, Phys. Rev. Lett. **88**, 017004 (2002).

<sup>3</sup> I. J. Lee, M. J. Naughton, G. M. Danner, and P. M. Chaikin, Phys. Rev. Lett. **78**, 3555 (1997).

<sup>4</sup> S. Belin and K. Behnia, Phys. Rev. Lett. **79**, 2125 (1997).

<sup>5</sup> M. Takigawa, H. Yasuoka, and G. Saito, Journ. Phys. Soc. Japan **56**, 873 (1987).

<sup>6</sup> I. J. Lee, A. P. Hope, M. J. Leone, and M. J. Naughton, Synth. Metals **70**, 747 (1995).

<sup>7</sup> I. J. Lee and M. J. Naughton, "The Superconducting State in Magnetic Fields: Special Topics and New Trends", Ed. C. A. R. Sá de Melo, Ch. 14, pp. 272-295, World Scientific, Singapore (1998).

<sup>8</sup> A. A. Abrikosov, J. Low Temp. Phys. **53**, 359 (1983).

<sup>9</sup> A. G. Lebed, JETP Lett. **44**, 114 (1986).

<sup>10</sup> N. Dupuis, G. Montambaux, and C. A. R. Sá de Melo, Phys. Rev. Lett. **70**, 2613 (1993).

<sup>11</sup> C. A. R. Sá de Melo, Physica C **260**, 224 (1996).

<sup>12</sup> A. G. Lebed, K. Machida, M. Ozaki, Phys. Rev. B **62**, R795 (2000).

<sup>13</sup> H. Shimahara, Phys. Rev. B **61**, R14936 (2000).

<sup>14</sup> K. Kuroki, R. Arita, and H. Aoki, Phys. Rev. B **63**, 094509 (2001).

<sup>15</sup> R. D. Duncan, C. D. Vaccarella, and C. A. R. Sá de Melo, Phys. Rev. B **64**, 172503 (2001).

<sup>16</sup> R. D. Duncan, R. W. Cherg, and C. A. R. Sá de Melo, cond-mat/0203570 (2002).

<sup>17</sup> C. A. R. Sá de Melo, "The Superconducting State in Magnetic Fields: Special Topics and New Trends", Ch. 15, p. 318, World Scientific, Singapore (1998).

<sup>18</sup> C. A. R. Sá de Melo J. Supercond. **12**, 459 (1999).

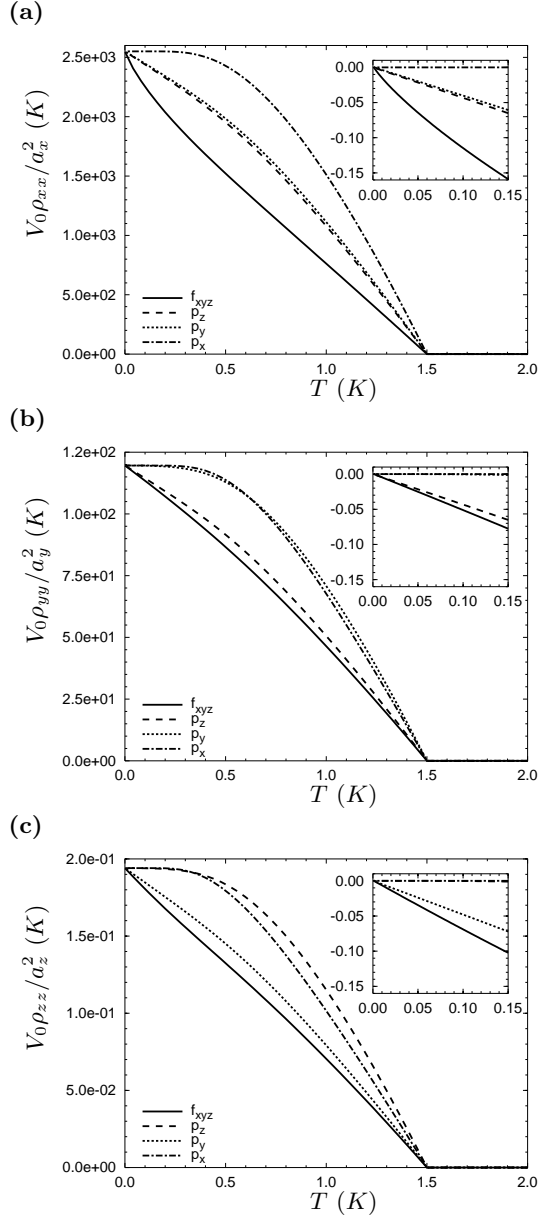


FIG. 4: Temperature dependence of  $V_0 \rho_{ii} / a_i^2$  in thermal units (K).  $V_0$  ( $a_i$ ) is the unit cell volume (length). Insets show the low  $T$  behavior of  $\Delta \rho_{ii} \equiv [\rho_{ii}(T) / \rho_{ii}(0) - 1]$ .